

Supplementary Information

**Enhancement of thermal stability of *Bacillus subtilis*  
168 glycosyltransferase YjiC based on PoPMuSiC  
algorithm and its catalytic conversion of rare  
ginsenoside PPD**

**Hua Guo<sup>1</sup>, Weina Li<sup>1,\*</sup>, Chenhui Zhu<sup>1</sup>, Yanru Chen<sup>1</sup>, Paul A. Dalby<sup>2</sup>, Daidi Fan<sup>1,\*</sup>**

<sup>1</sup>Shaanxi Key Laboratory of Degradable Biomedical Materials, Shaanxi R&D Center of Biomaterials and Fermentation Engineering, Biotech. & Biomed. Research Institute, School of Chemical Engineering, Northwest University, Shaanxi 710069, China.

<sup>2</sup>Department of Biochemical Engineering, UCL, London WC1E 6BT, UK.

\*Corresponding Authors:

Address: School of Chemical Engineering, Northwest University, 229 North Taibai Road, Xi'an 710069, Shaanxi, China.

Weina Li, Tel: +86-29-88305118, Fax: +86-29-88305118, E-mail: [liweina@nwu.edu.cn](mailto:liweina@nwu.edu.cn)

Daidi Fan, Tel: +86-29-88305118, Fax: +86-29-88305118, E-mail: [fandaidi@nwu.edu.cn](mailto:fandaidi@nwu.edu.cn)

Table S1 A list of oligonucleotides used in this study.

Primer	Sequence <sup>a</sup> (5'→3')
E52V_F	GT <u>GTGG</u> CACTGATTTATCATACCTCTC
E52V_R	CTATTTAGTCAC <u>GGTGTGG</u> CGG
K65G_F	CC <u>GGCC</u> CAGATTCGTGAAATG
K65G_R	GTAAAGTGCTTAGAC <u>CGGG</u> CC
D75V_F	GATGGAAAAAAT <u>GTGG</u> CACCG
D75V_R	GAGTCGCCAC <u>GGTGT</u> AAAAAAG
L78H_F	GAAAAAATGATGCACCG <u>CAC</u> AG
L78H_R	GTCCGAC <u>CAC</u> GCCACGTAG
P89R_F	GCATTCTG <u>CGT</u> CAGCTGGAAGAAC
P89R_R	CAAGAAGGTCGACT <u>TGCGT</u> CTTACGAG
K125I_F	CTGAATGTTCCGGTTATT <u>ATT</u> CTGTG
K125I_R	GTGTGTT <u>ATT</u> ATTGGCCTTGTAAGTC
E141P_F	CAGCTGGGTAAT <u>CCGG</u> ATATG
E141P_R	GTCGTATAG <u>GCCT</u> AATGGGTC
E159P_F	CATATCTG <u>CCGC</u> CAGGAAAAAC
E159P_R	GTCAAAAAGGAC <u>GCC</u> GTC
E175P_F	GTTCCG <u>CCGC</u> CACTGAATATTG
E175P_R	GTATTTTTGTTATAAGTCACG <u>GCCGC</u>
N178I_F	CGGCATAAAAACA <u>AATA</u> ATCAGTGCTTCCG
N178I_R	CCGTCAAGGCCTTCGTGACTA <u>AATA</u> AC
S203I_F	GTTTTGTTGGTCCG <u>ATC</u> CTG
S203I_R	GTGGGTC <u>CTAG</u> CCTGGTTG
E209P_F	GAACGTAAAC <u>CCG</u> AAAGAAAGCCTG
E209P_R	GTTAGTCGTCCGAAAGAAAG <u>GCC</u>
L214E_F	CTG <u>GAA</u> ATTGATAAAGATGATCGTCCGC
L214E_R	GCTAGTAGAAATAGTTA <u>AAAG</u> GTCCGAAAG
P313W_F	GGTTGTTATT <u>TGGC</u> CAGATGTATGAACAGG
P313W_R	TGTAGAC <u>GGT</u> TTATTGTTGGTCGCCTTC
K336P_F	<u>GCCG</u> CCGGAAGAAGTTACC
K336P_R	<u>CCGG</u> CGGCAGATAAACACC
D367M_F	CAGAAA <u>ATGG</u> TAAAGAAGCAGGTGG
D367M_R	GGTGGACGAAGAAATTG <u>GTA</u> AAAGAC

<sup>a</sup> The mutated bases are underlined

**Table S2.** The selected single-site mutants and their folding free energy ( $\Delta\Delta G$ ) values

based on the PoPMuSiC 2.1 algorithm.

Mutants	$\Delta\Delta G$	Mutants	$\Delta\Delta G$
E52V	-0.78	E175P	-0.72
K65G	-0.72	N178I	-1.56
D75V	-0.69	S203I	-0.81
L78H	-0.75	E209P	-0.94
P89R	-0.97	L214E	-0.58
K125I	-1.67	P313W	-1.79
E141P	-0.46	K336P	-0.89
E159P	-0.90	D367W	-0.42

**Table S3.** Heat-sensitive residues of the WT and variants

Enzyme	Regions of heat-sensitive residues
WT	4, 48-63, 65, 68-89, 91, 113, 118, 119, <u>123-139</u> , 152, 154-157, 172-174, <u>177-190</u> , 192, 193-196, 211, 213-215, 272, 318, 321, 347-348, 350-352, 356-367, 369, 372-388
K125I	18-19, 22, 25-26, 56-57, 59-69, 81, 83-95, 97, <u>113-139</u> , 147-153, 156, 159, 161-164, 168-169, 217, 235, 245-247, 266-277, 341-348, 378-388
K125I/N178I	60-62, 132-133, 135-141, 143-145, 162-166, 168, 186-193, 214, 230-232, 234, 236-251, 257-276, 316-317, 320-321, 324-342, 361-388
M315F	4, 49, 66-68, 71-78, 122, <u>124-141</u> , 143-160, 171, 175, 181, 186-204, 207, 215, 217, 237, 269-272, 296-297, 299-325, 327-330, 338-367, 373-375, 377-388

Sequence optimality (sum of negative ddG per sequence position) - yjiC.pdb - Systematic - 06-05-2022

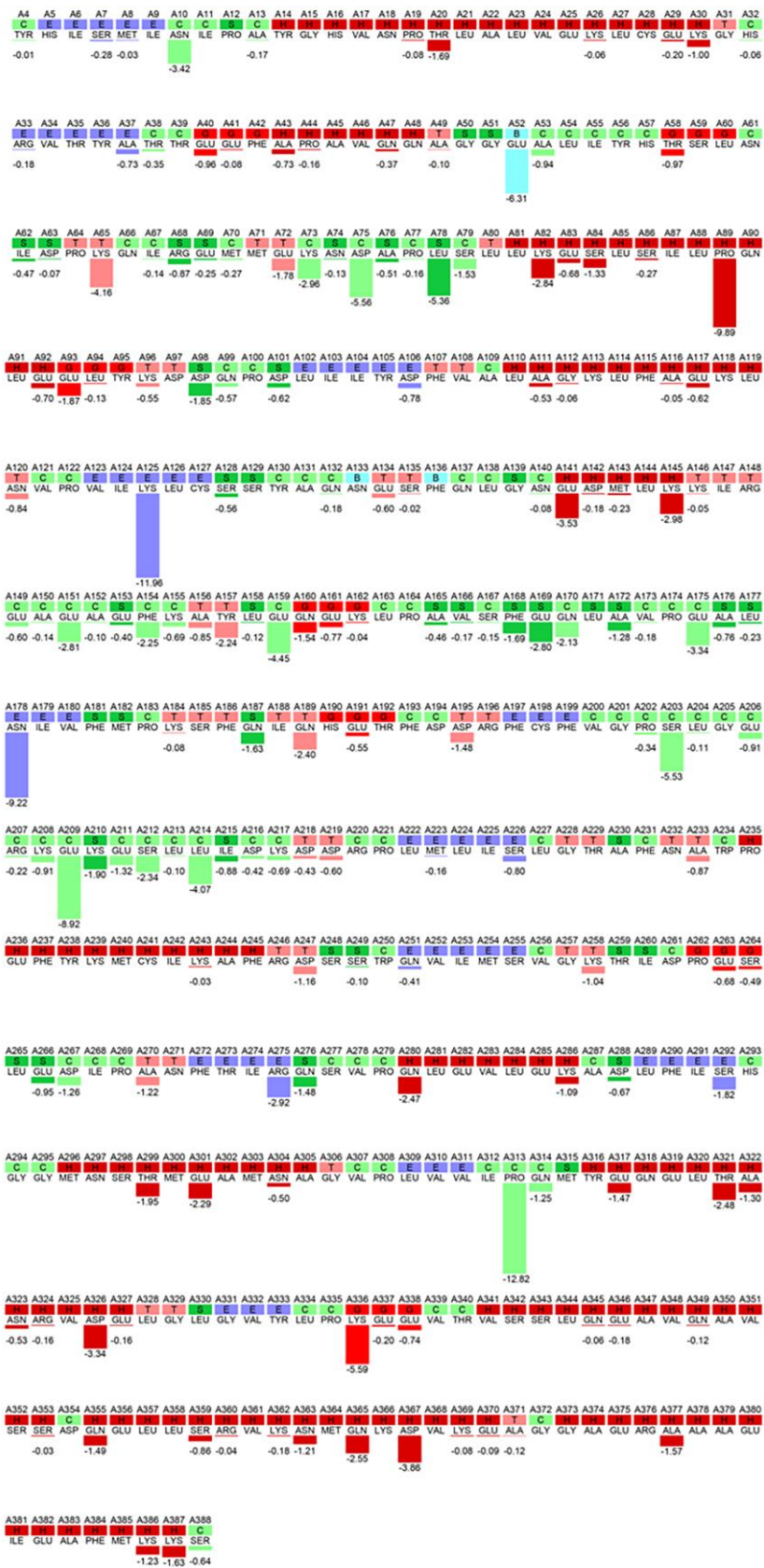
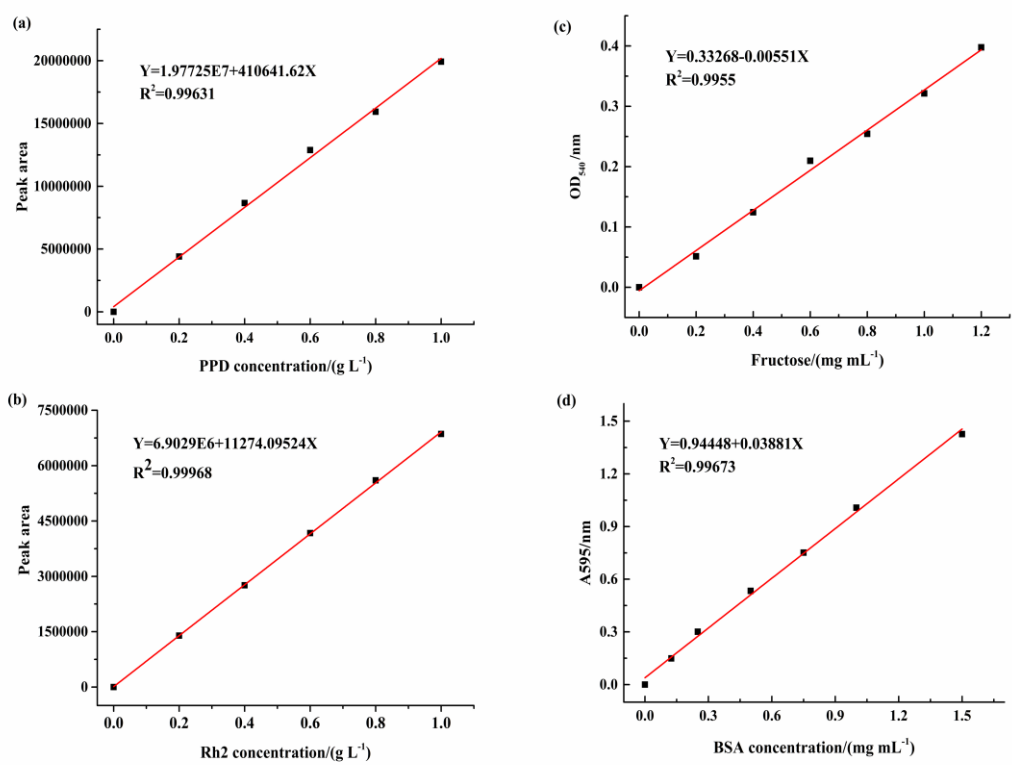
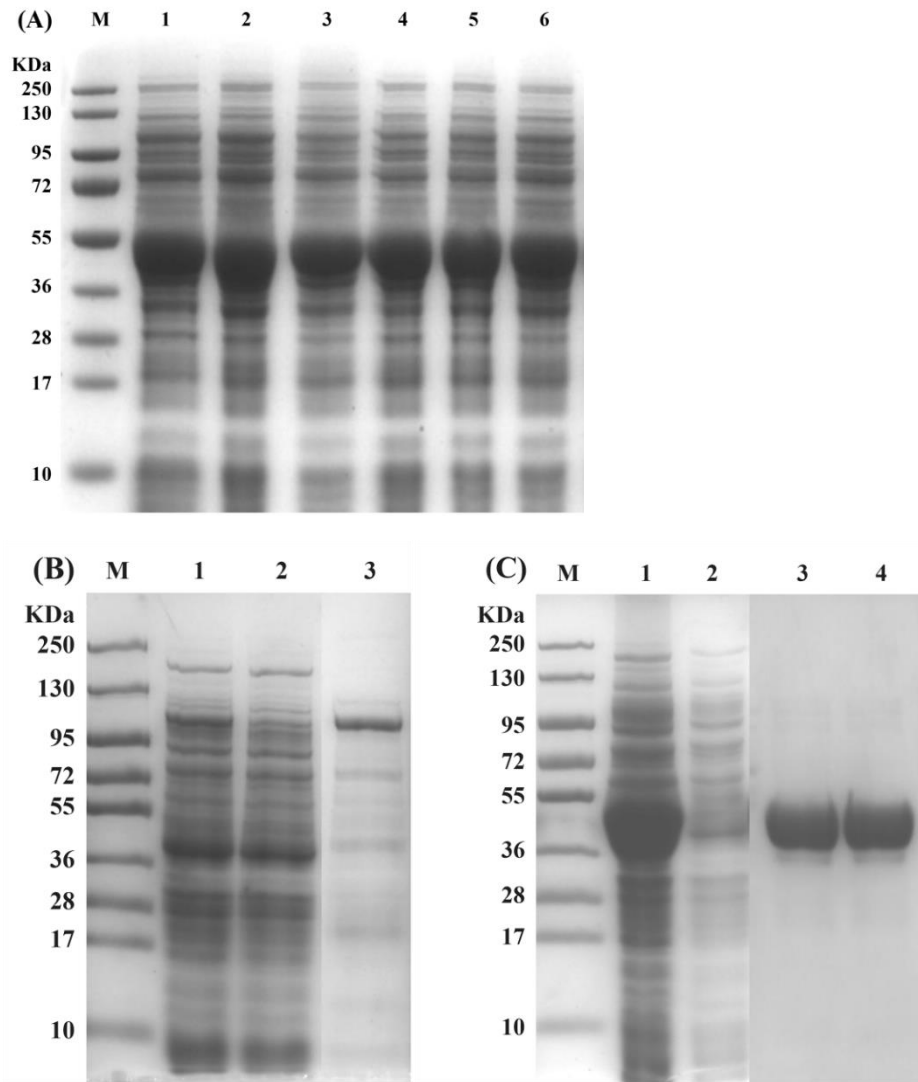


Figure S1. The analysis of the BS-YjiC protein structures by PoPMuSiC.



**Figure S2.** Standard curve. (a) ginsenoside PPD, (b) ginsenoside Rh2, (c) fructose, (d) BSA.



**Figure S3.** SDS-PAGE (8%) analysis of Bs-YjiC and AtSuSy expressed in *E. coli* BL21 (DE3). (A) SDS-PAGE analysis of Bs-YjiC and its mutants. M: marker, line 1, WT; line 2, K125I; line 3, N178I; line 4, P313W; line 5, K125I/N178I; and line 6, K125I/P313W. (B) SDS-PAGE analysis of AtSuSy. M: marker, line 1, Crude AtSuSy after cell fragmentation; line 2, Crude AtSuSy which was not induced; line 3, AtSuSy purified by Ni-NTA column. (C) SDS-PAGE analysis of Bs-YjiC and its mutants. M: marker, line 1, Crude Bs-YjiC after cell fragmentation; line 2, Crude Bs-YjiC which was not induced; line 3, WT purified by Ni-NTA column; line 4, K125I/E178I purified by Ni-NTA column.

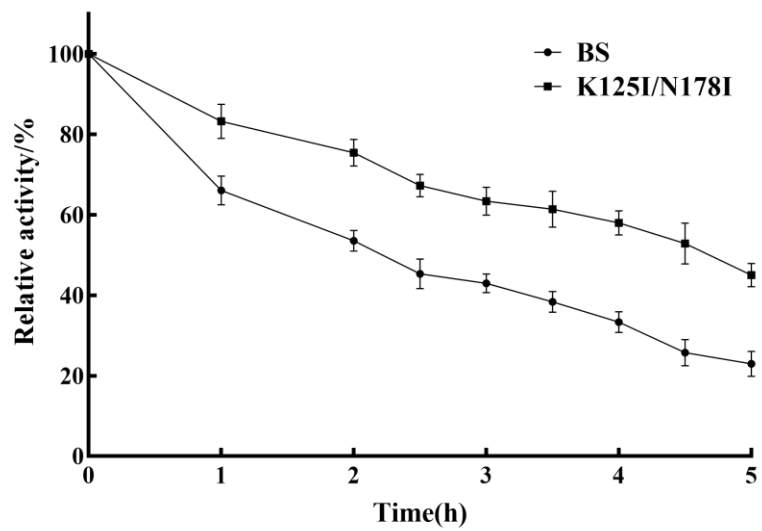


**Figure S4.** Thermostability of BS-YjiC and its mutants at 55 °C.



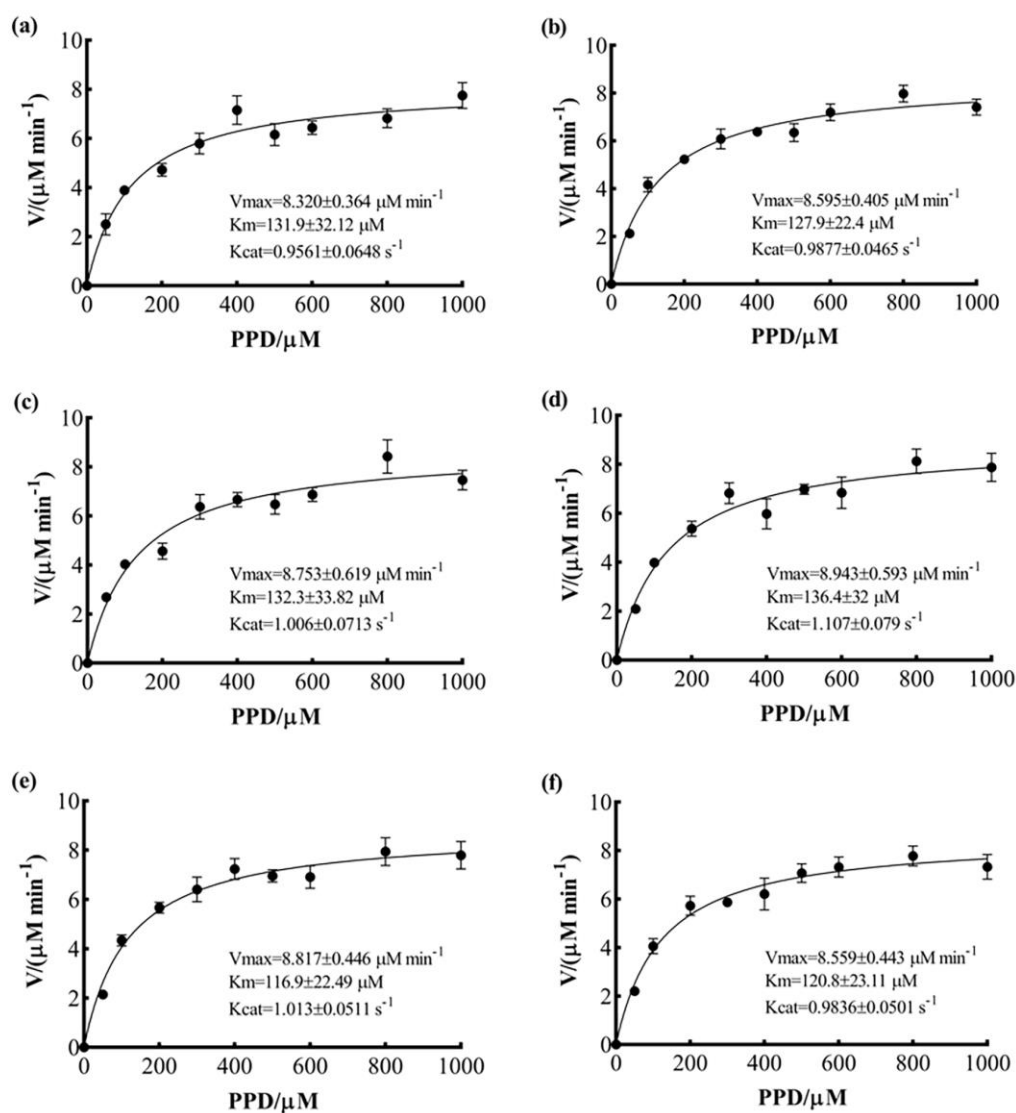


**Figure S5.** Kinetic plot of the enzymatic reactions to ginsenoside PPD. (a) WT, (b) K125I, (c) N178I, (d) P313W, (e) K125I/N178I, (f) K125I/P313W.

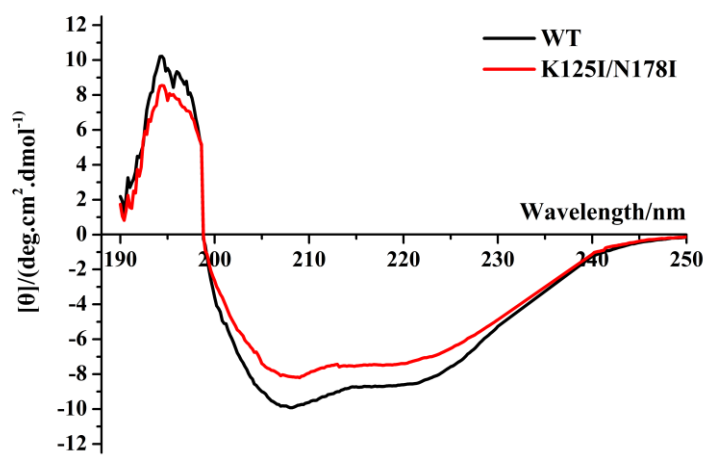


**Figure S6.** CD spectra of WT and mutant K125I/N178I glycosyltransferase.

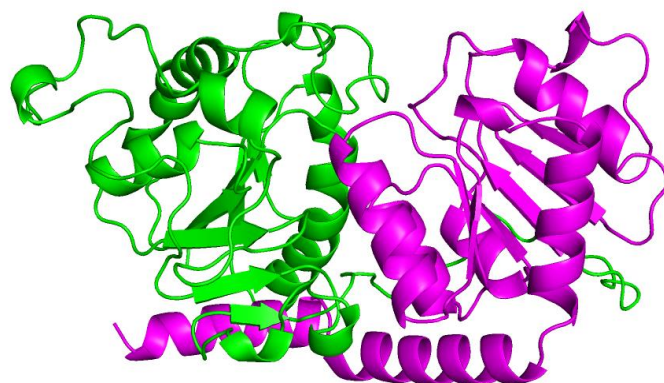


**Figure S7.** Overall structure of the Bs-YjiC displayed with PYMOL. The N-terminal and C-terminal domains are marked in green and magenta, respectively.

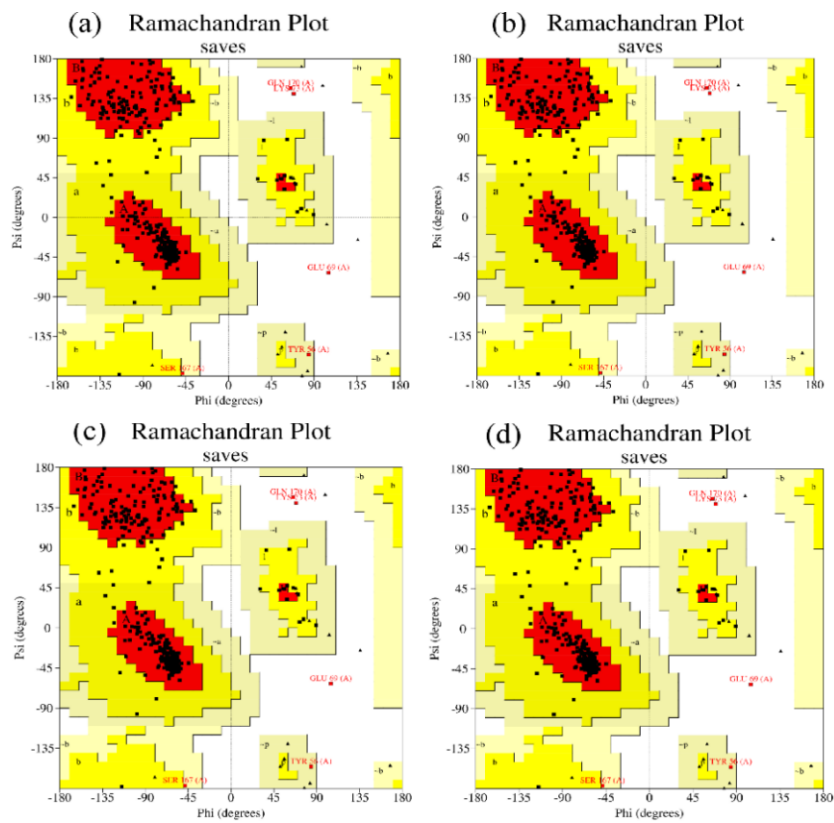


**Figure S8.** Ramachandran plots of YjiC and its mutants. (a) WT, (b) K125I, (c) N178I, (d) K125I/N178I. Residues in the most favored regions are displayed in red. Residues in additionally allowed regions are presented in yellow.

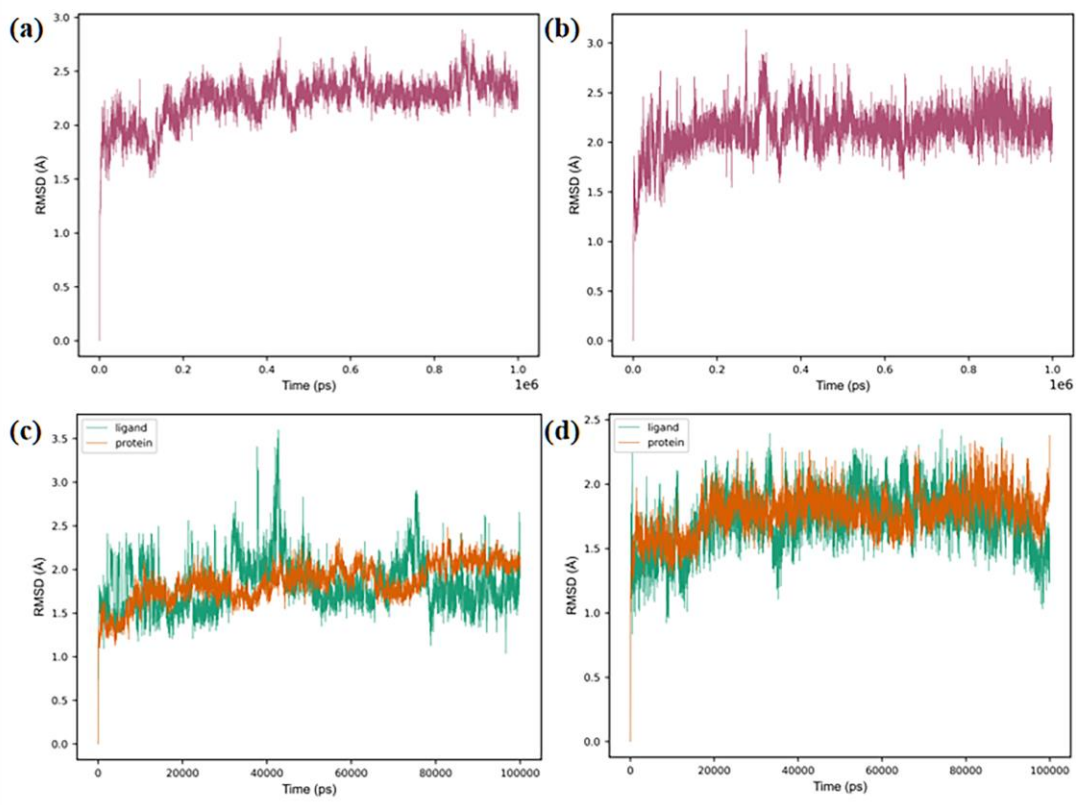


**Figure S9.** RMSD of the BS-YjiC-ligand complexes. (a) WT, (b) ligand, (c) WT-ligand complex, (d) mutant K125I/N178I-ligand complex.

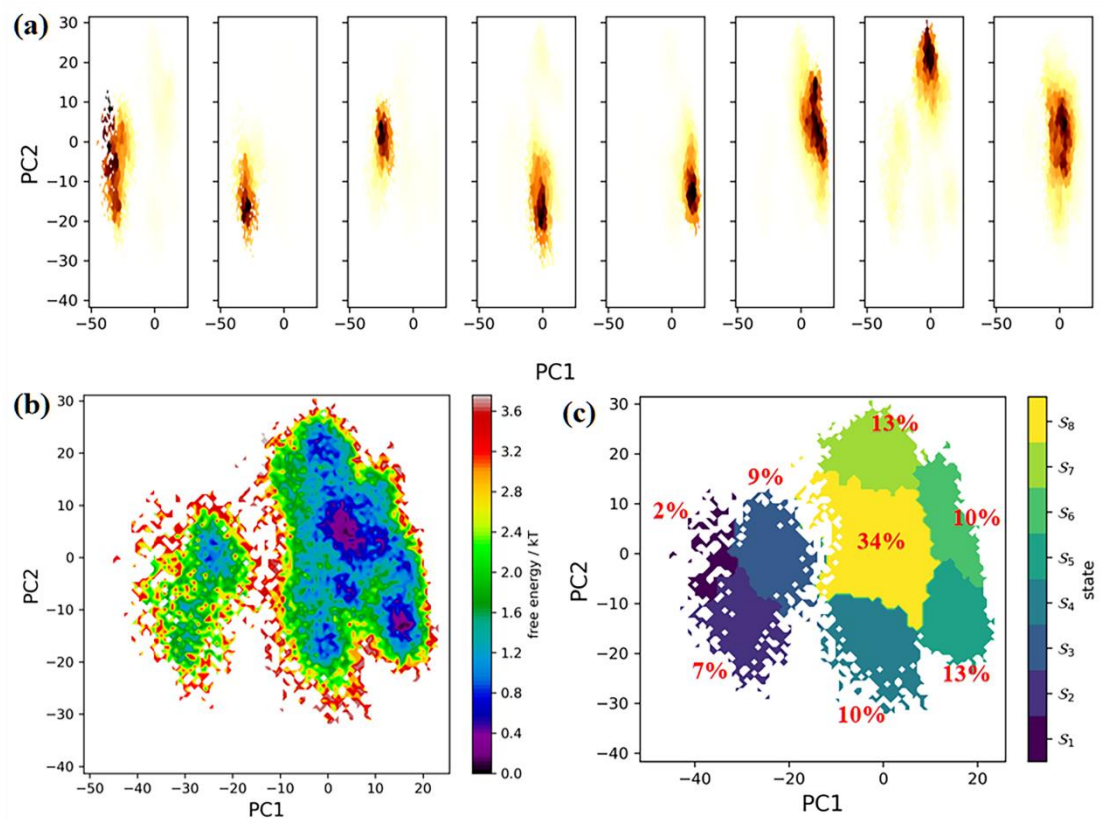


**Figure S10.** Principal component analysis (PCA) of Markov chain model (MSM). (a) multiple, (b) Free energy surface (FEL), (c) states.

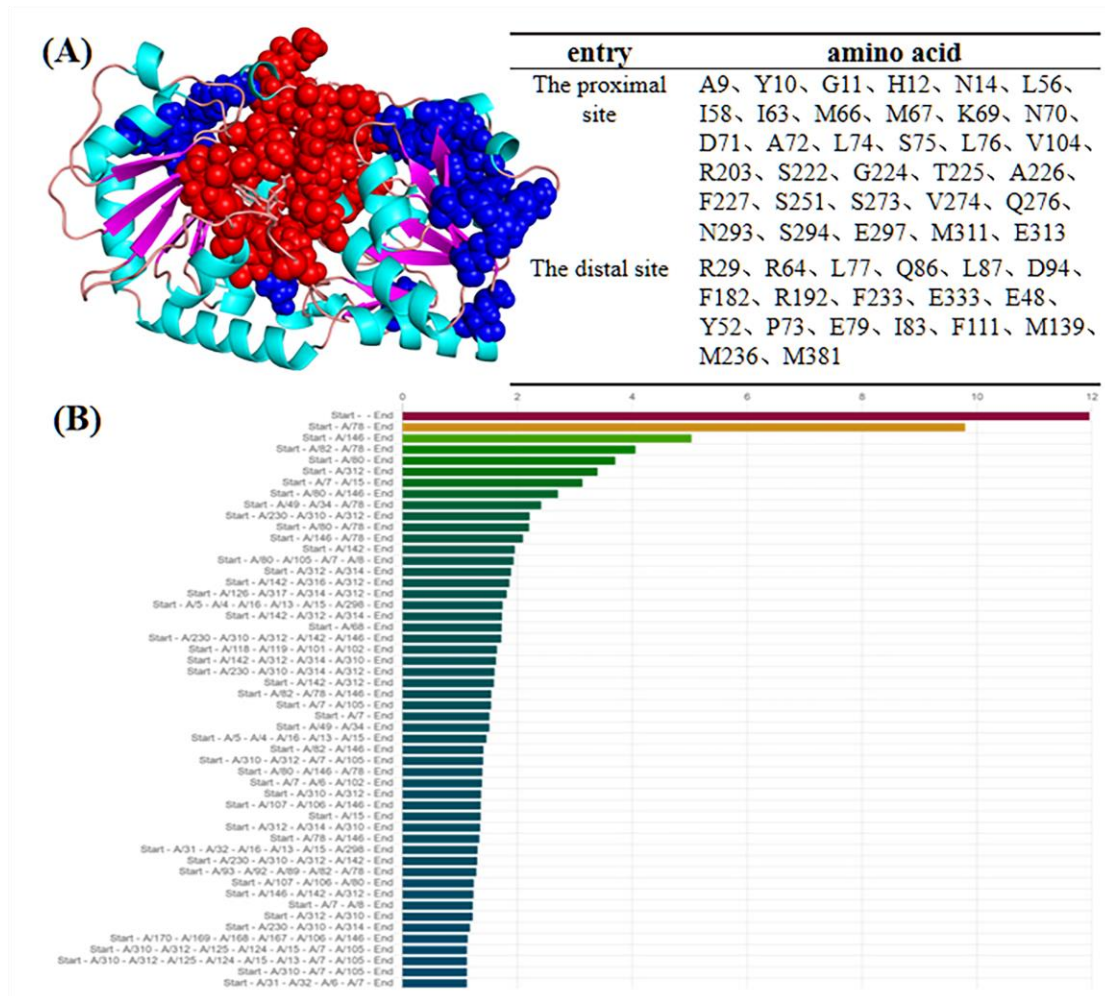


**Figure S11.** Distal effect pathway. (A) Red represents the proximal site, blue represents the distal site. (B) The weighting proportion here refers to the importance of each path in the signal transduction pathway (Due to Pymol counting issues, the actual amino acid ranking should be +1). The higher the weight, the more important the role of this path in the entire regulatory process.

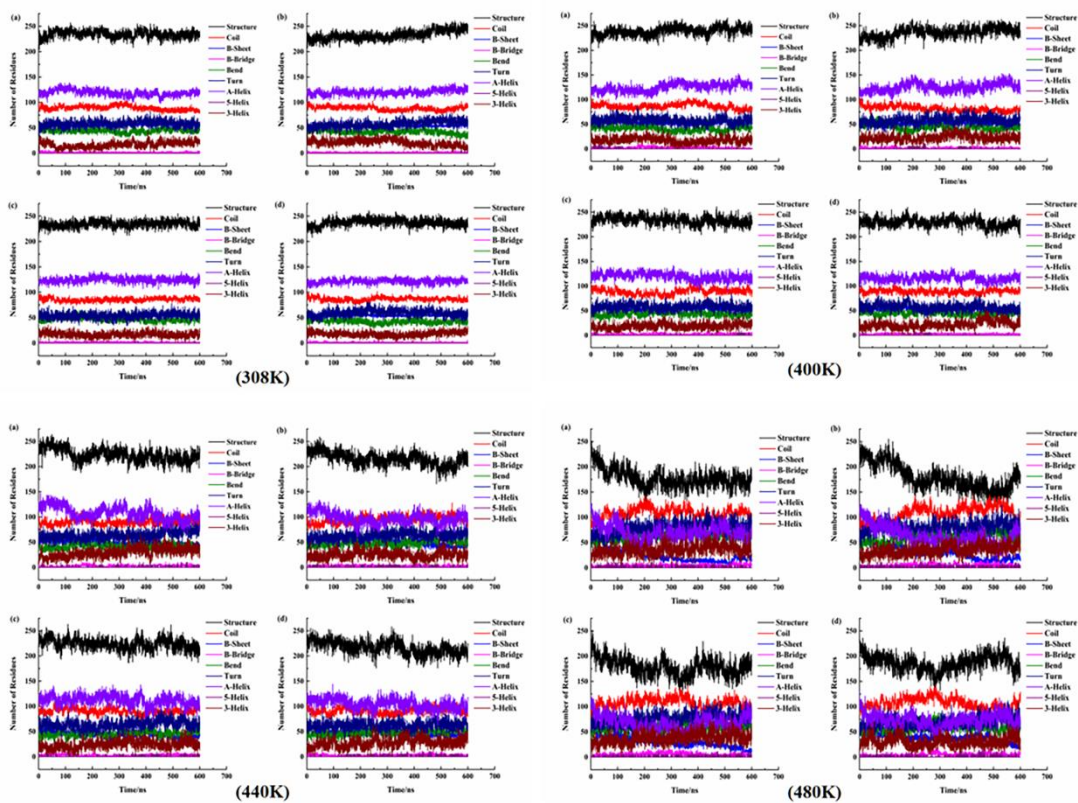


**Figure S12.** Secondary structure development trajectories of BS-YjiC and its mutants (K125I, K125I/N178I and M315F) at different temperatures. Different secondary structure elements are displayed by colors at the figure's bottom. (a) 308K, (b) 400K, (c) 440K, (d) 480K.



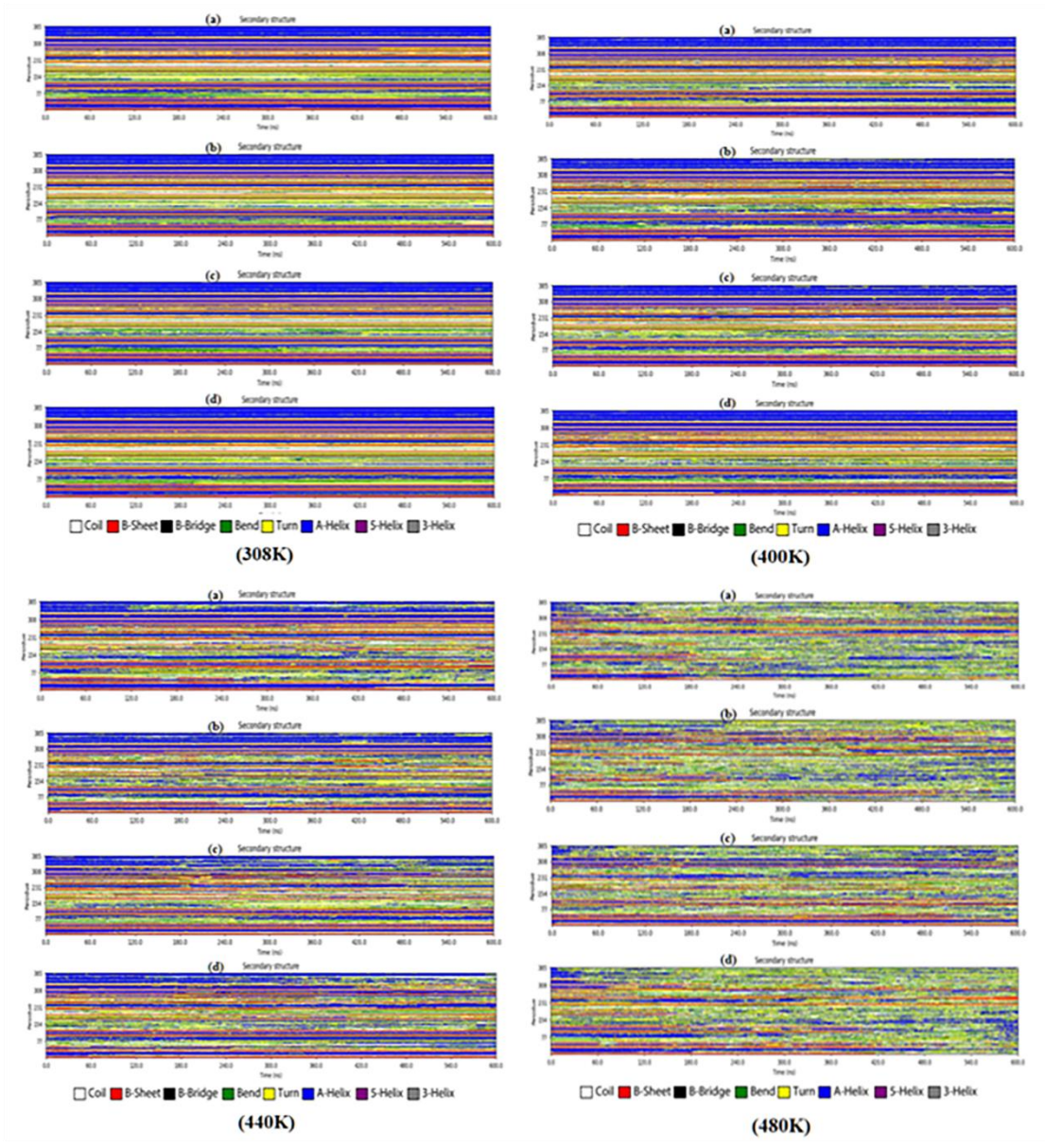


**Figure S13.** Development trajectories of secondary structure elements of BS-YjiC and its mutants (K125I, K125I/N178I and M315F) at different temperatures. (a) 308K, (b) 400K, (c) 440K, (d) 480K.

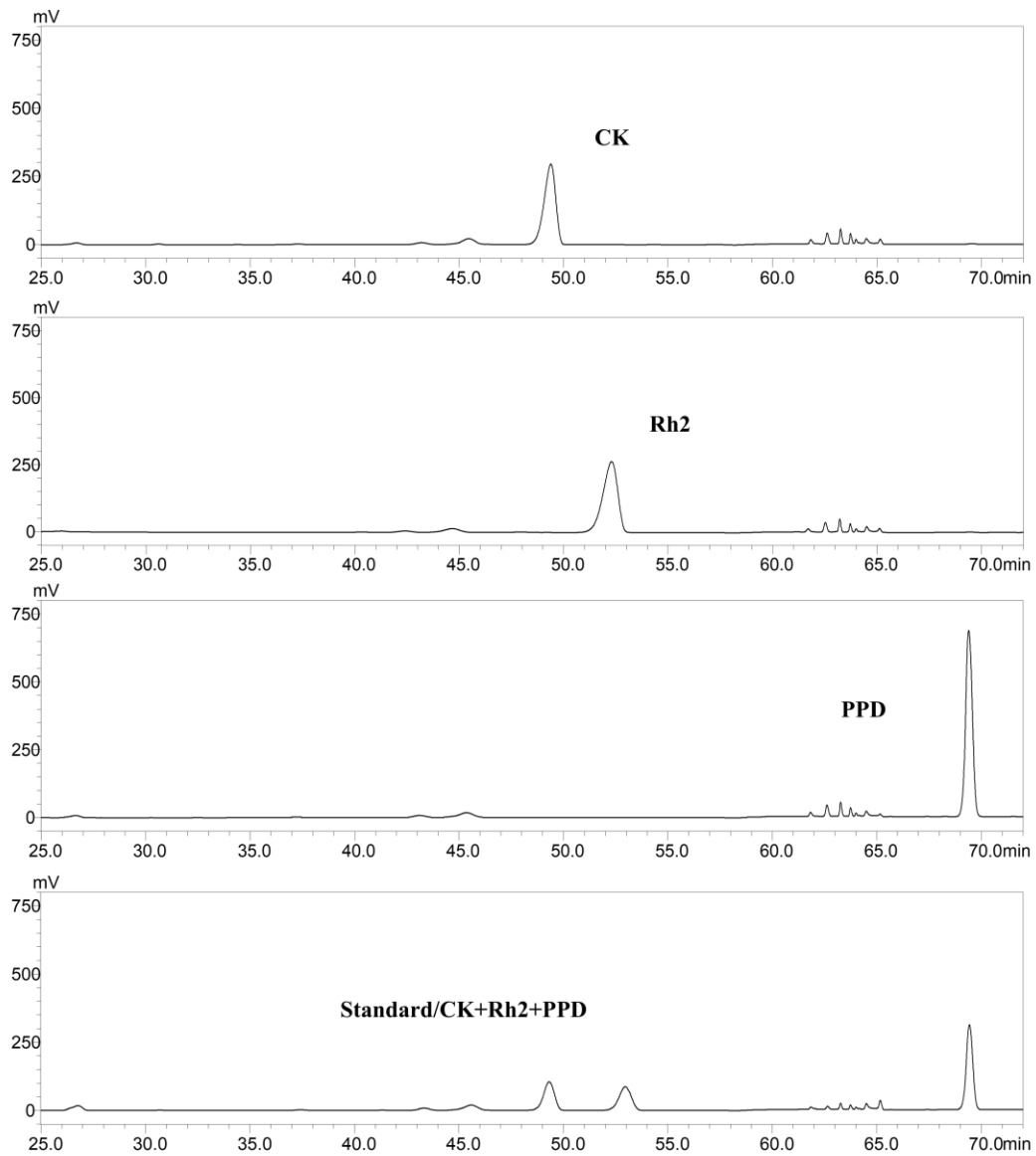


**Figure S14.** HPLC chromatogram of the Standard ginsenosides.

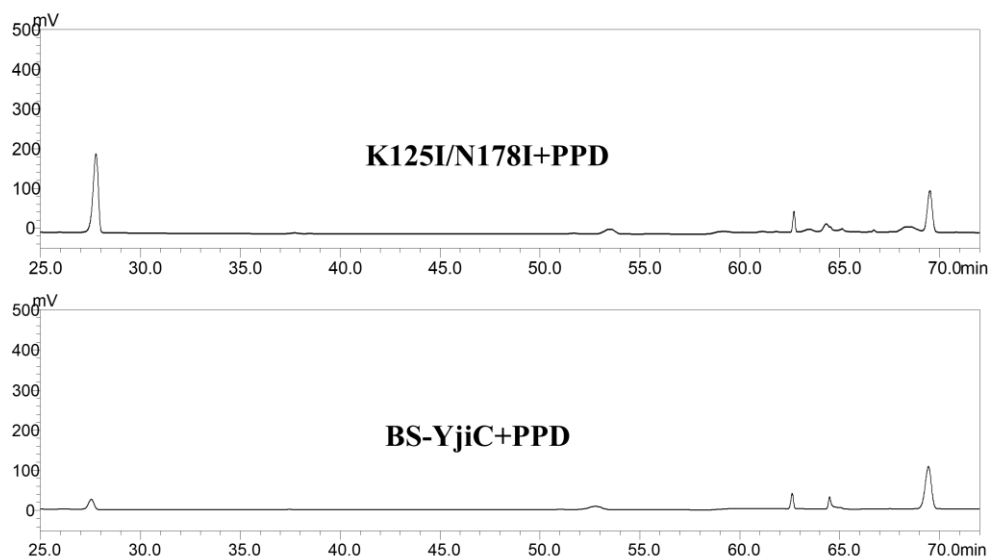


**Figure S15.** HPLC chromatogram of the BS-YjiC and the mutant K125I/N178I reacted with PPD at 45 °C, respectively.

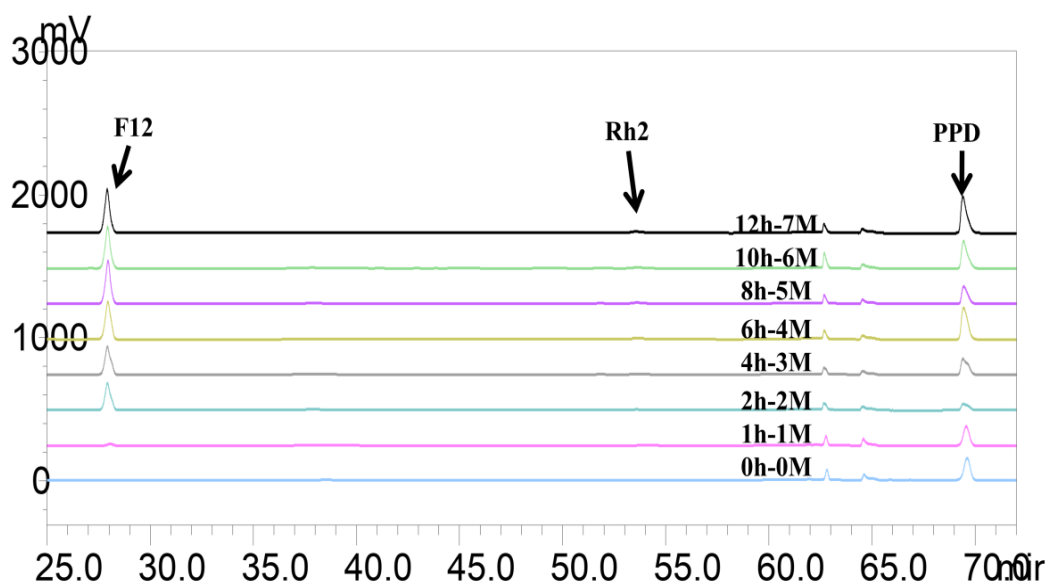


**Figure S16.** HPLC chromatograms of reaction products of the mutant K125I/N178I-AtSuSy cascade. The reaction system (20 mL) contained 1 mM PPD, 0.25 mM UDP, 50 mM Tris-HCl (pH 8.0), 0.5 M sucrose, 6% DMSO, 100 mU mL<sup>-1</sup> Bs-YjiC and 240 mU mL<sup>-1</sup> AtSuSy. The reaction was conducted at 45 °C for 14 hours. 100 µL of PPD (200 mM) was added to the reaction mixture at 1, 2, 4, 6, 8, and 10 h, respectively. Fresh enzymes (100 mU mL<sup>-1</sup> Bs-YjiC and 240 mU mL<sup>-1</sup> AtSuSy) were added at 4 and 8h.

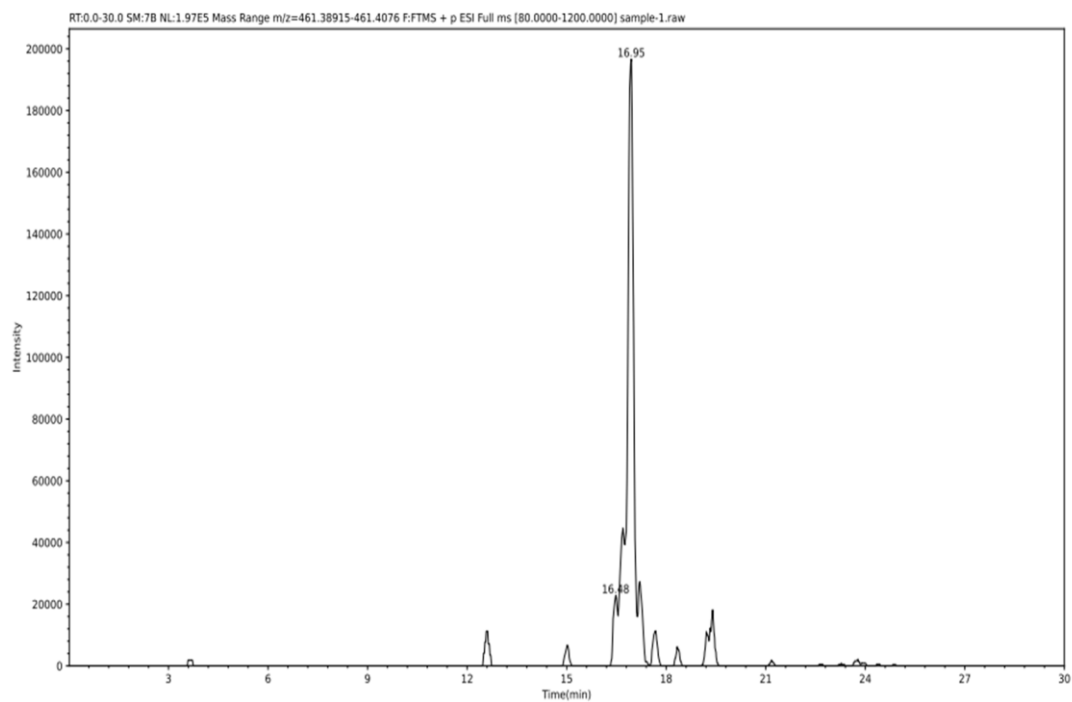


**Figure S17.** LC-MS spectrum of PPD ( $C_{30}H_{52}O_3$ ; calculated molecular weight:  $[M+H]^+ = 461.39837$ , DMSO- $d_6$ ).

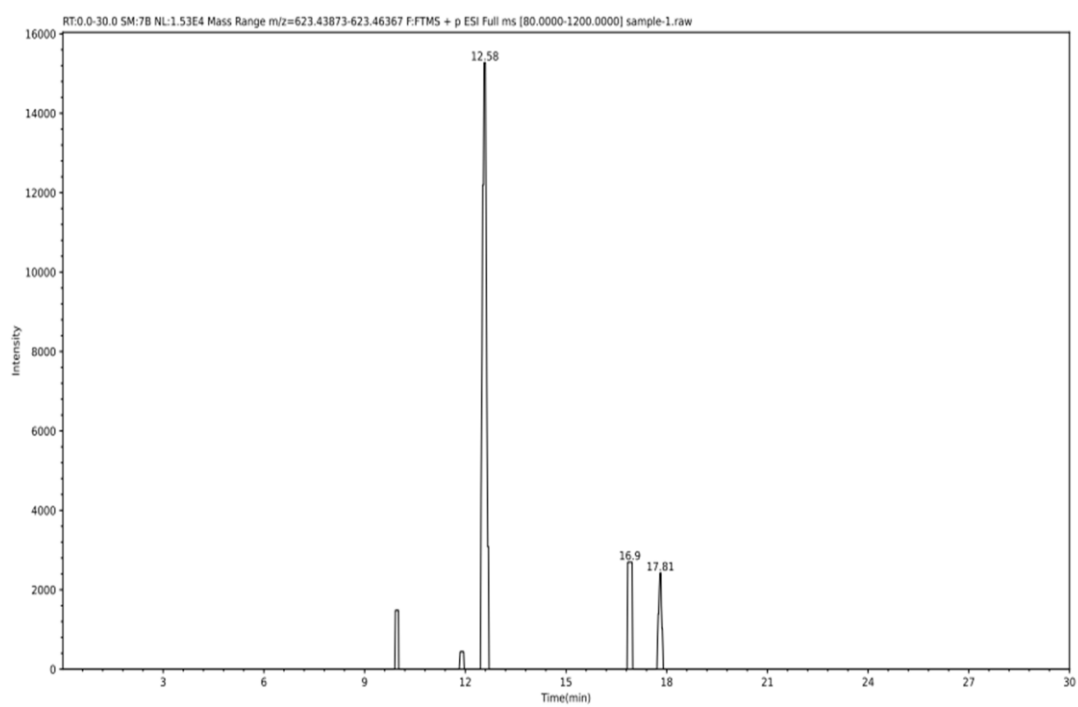


**Figure S18.** LC-MS spectrum of Rh2 ( $C_{36}H_{62}O_8$ ; calculated molecular weight:  $[M+H]^+ = 623.45120$ , DMSO- $d_6$ ).

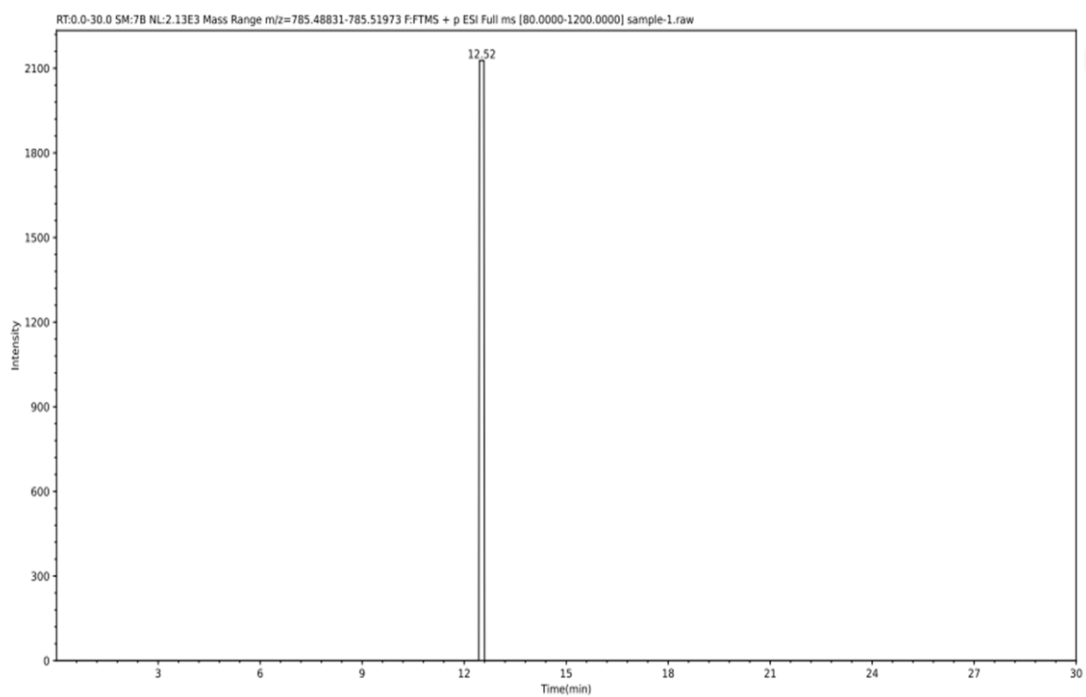


**Figure S19.** LC-MS spectrum of F12 ( $C_{42}H_{72}O_{13}$ ; calculated molecular weight:  $[M+H]^+ = 785.50402$ , DMSO- $d_6$ ).